Histol Histopathol (2022) 37: 863-877

http://www.hh.um.es

Histology and Histopathology
From Cell Biology to Tissue Engineering

ORIGINAL ARTICLE **Open Access**

CircRNA circBACH1 facilitates hepatitis B virus replication and hepatoma development by regulating the miR-200a-3p/MAP3K2 axis

Na Du[1]*, Kailin Li[1]*, Yu Wang[2], Bo Song[1], Xuan Zhou[1] and Shaoqiong Duan[1]

[1]Department of Infectious Disease and [2]Department of Cardiology, Suizhou Central Hospital Affiliated to Hubei Medical College, Suizhou, China

*These authors contributed equally to this paper

Summary. Background. Hepatitis B virus (HBV) is a top contributor to hepatoma. Circular RNAs (circRNAs) have been elucidated to have a close connection with HBV-induced hepatoma. This study aimed to explore the role of circRNA BTB domain and CNC homolog 1 (circBACH1) in HBV replication and hepatoma progression, as well as the potential mechanistic pathway.

Methods. Quantitative real-time polymerase chain reaction (qRT-PCR) assay was performed to assess the expression of circBACH1, microRNA (miR)-200a-3p, and mitogen-activated protein kinase kinase kinase 2 (MAP3K2). HBV replication was determined by enzyme-linked immunosorbent assay (ELISA) and qRT-PCR assay. Cell viability and clonogenicity were detected via Cell Counting Kit-8 (CCK-8) assay and colony formation assay, respectively. Cell metastasis was examined by Transwell assay and wound healing assay. Annexing-V/PI staining was employed to monitor cell apoptosis using flow cytometry. Levels of MAP3K2, proliferation- and apoptosis-related proteins were analyzed by Western blotting. Target interaction between miR-200a-3p and circBACH1 or MAP3K2 was confirmed by dual-luciferase reporter assay and RNA immunoprecipitation (RIP) assay. The role of circBACH1 *in vivo* was investigated by xenograft model assay.

Results. Expression of circBACH1 and MAP3K2 was increased, while miR-200a-3p expression was decreased in HCC tissues and HBV-transfected hepatoma cells. Depletion of circBACH1 or miR-200a-3p overexpression impeded HBV replication, proliferation, and metastasis in HBV-transfected hepatoma cells. CircBACH1 was able to regulate MAP3K2 expression by sponging miR-200a-3p. CircBACH1 regulated HBV replication and hepatoma progression through the miR-200a-3p/MAP3K2 pathway. Moreover, circBACH1 deficiency hampered tumor growth *in vivo*.

Conclusion. CircBACH1 knockdown had inhibitory effects on HBV replication and hepatoma progression, at least partly by modulating the miR-200a-3p/MAP3K2 axis.

Key words: Hepatoma, HBV replication, circBACH1, miR-200a-3p, MAP3K2

Introduction

Hepatoma remains one of the most prevalent malignancies all over the world, triggering one million new cases and 7×10^5 deaths per year, and its 5-year survival rate is low (Balogh et al., 2016). Hepatocellular carcinoma (HCC) ranks as the most common liver cancer, whose initiation is chiefly attributed to infection with Hepatitis B virus (HBV) (Fares and Peron, 2013). HBV is a hepatotropic virus that attacks approximately 3.5% of people worldwide (Yuen et al., 2018). After viral infection, HBV continues to replicate. And covalently closed circular DNA (cccDNA) is vital for HBV persistent infection (Sun et al., 2018). Therefore, further exploration of HBV replication might be helpful for developing a novel drug for HBV treatment.

Circular RNAs (circRNAs) can be back-spliced from exons of linear RNAs, with high abundance in the eukaryotic transcriptome and diverse biological functions in eukaryotic cells (Qu et al., 2015). Due to the special covalently closed loop shape, circRNAs are more resistant to RNA enzyme degradation (Chen, 2016). CircRNAs have been documented to have diverse roles in hepatoma cell proliferation, apoptosis, and

Corresponding Author: Shaoqiong Duan, Department of Infectious Disease, Suizhou Central Hospital Affiliated to Hubei Medical College, No. 8, Wendi Avenue, High-tech Zone, Zengdu District, Suizhou 441300, China. e-mail: duanshaoqiong1983@163.com

DOI: 10.14670/HH-18-452

metabolism (Song et al. 2018). In addition, certain circRNAs also have an association with HBV-related liver cancers (Cui et al., 2018). Derived from the BTB domain and CNC homolog 1 (BACH1) gene, circBACH1 was identified to exert an oncogenic role in HCC progression (Liu et al., 2020). Whether circBACH1 is involved in HBV replication remains to be explored.

MicroRNAs (miRNAs) are small non-coding RNAs that alter gene expression by complementarily binding to 3' untranslated region (3'UTR) of involved target genes, thereby participating in cancer progression (Lai, 2002; Paulmurugan, 2013). Furthermore, many miRNAs exert a tumor-suppressing role in HBV-related HCC, like miR-29c (Wang et al., 2011), miR-152 (Huang et al., 2010), and miR-22 (Jiang et al., 2011). Shi et al. alleged that miR-200a-3p could impede the malignant properties of HBV-positive cells (Shi et al., 2017). In this paper, Starbase 3.0 analysis forecasted that miR-200a-3p was a possible target of circBACH1. However, the association between miR-200a-3p and circBACH1-mediated HBV replication is unclear.

Mitogen-activated protein kinase kinase kinase 2 (MAP3K2) is a member of the serine/threonine-protein kinase family, which is involved in the growth of several human tumors, including non-small cell lung cancer (Huang et al., 2016), breast cancer (Wang and Wen, 2020), cutaneous malignant melanoma (Chen et al., 2019b), neuroblastoma (Zhu et al., 2021), and HCC (Zhang et al., 2021). Moreover, MAP3K2 participates in miR-122-mediated inhibitory impact on hepatoblastoma cell migration and HBV replication (Chen et al., 2019a). MAP3K2 was estimated to be a target gene of miR-200a-3p. Regrettably, evidence on the connection between miR-200a-3p and MAP3K2 in HBV replication is scarce.

In this work, the expression of circBACH1 in HCC tissues and HBV-transfected hepatoma cells was detected. The effects of circBACH1 on HBV replication and hepatoma development were investigated. The molecular mechanism by which circBACH1 functioned in hepatoma cells was also explored.

Materials and methods

Collection of clinical specimens

Thirty-one HCC tissues and paired adjacent healthy tissues were procured from Suizhou Central Hospital Affiliated to Hubei Medical College. Tissues were collected from HCC patients during surgery, and all patients submitted written informed consent. This study was ethically ratified by the Ethics Committees of Suizhou Central Hospital Affiliated to Hubei Medical College.

Cell culture and HBV infection

Hepatoma cell lines HepG2 and Huh7 (CL-0120; Procell, Wuhan, China), as well as 293T cells (CRL-1573; American Type Culture Collection, Manassas, VA, USA) were cultivated in Dulbecco's Modified Eagle Medium (Thermo Fisher, Rockford, IL, USA) mixed with 10% fetal bovine serum (Gibco, Grand Island, NY, USA) and 1% penicillin/streptomycin (Gibco) in a humidified atmosphere containing 5% CO_2 at 37°C.

HepG2.2.15 and Huh7-1.3 cells were established by transfection of pHBV1.3 (plasmids containing the genomic sequence of HBV) into HepG2 and Huh7 cells, respectively (Zhang and Wang, 2020).

Cell transfection

Small interfering RNAs of circBACH1 si-circBACH1#1 (5'-GAG AAG CTG GTG ACA GTT AAA-3'), si-circBACH1#2 (5'-AGC TGG TGA CAG TTA AAG GAT-3') and si-circBACH1#3 (5'-AAG CTG GTG ACA GTT AAA GGA-3') were constructed to silence circBACH1 expression, with si-NC (5'-AAG TCG GGT CAA GAG AAG CTT-3') as a negative control, which all were furnished by GenePharma Co. Ltd. (Shanghai, China). MiR-200a-3p mimic (5'-ACA UCG UUA CCA GAC AGU GUU A-3'), miR-200a-3p inhibitor (5'-UGU AGC AAU GGU CUG UCA CAA U-3'), and their negative control: mimic NC (5'-UUU UCC GAA CGU UCA CGU TT-3') and inhibitor NC (5'-CUA ACG CAU GCA CAG UCG UAC G-3') were supplied by GeneCopoeia (Guangzhou, China). The overexpression plasmid of MAP3K2 (pcDNA-MAP3K2) was synthesized by cloning its complementary DNA (cDNA) sequence into pcDNA 3.1 vector (Invitrogen, Carlsbad, CA, USA), with an empty vector (pcDNA) as the negative control. Cell transfection assay was implemented with Lipofectamine 3000 (Invitrogen).

Quantitative real-time polymerase chain reaction (qRT-PCR)

Clinical specimens and cells were incubated with TRIzol reagent (Invitrogen) for isolating total RNA. The quality of RNA was measured with a NanoDrop ND-1000 spectrophotometer (Thermo Fisher). 1 μg RNA was subjected for cDNA synthesis with cDNA Reverse Transcription Kit (Applied Biosystems, Foster City, CA, USA) or miRNA Reverse Transcription Kit (Applied Biosystems), followed by qRT-PCR assay utilizing SYBR Green Master Mix (Applied Biosystems) or TaqMan MiRNA Assay Kit (Applied Biosystems). Relative expression was assessed by the $2^{-\Delta\Delta Ct}$ method (Livak and Schmittgen, 2001), and glyceraldehyde 3-phosphate dehydrogenase (GAPDH, for circBACH1, linear BACH1 and MAP3K2) or U6 (for miR-200a-3p) served as an internal control. Sequence information of qRT-PCR assay was as follows: circBACH1-forward (F), 5'-GCTGTCGCAAGAGAAAACTTG-3' and circBACH1-reverse (R), 5'-CCACACATTTGCAC ACTTCA-3'; linear BACH1-F, 5'-CACCGAAGGAG

ACAGTGAATCC-3' and linear BACH1-R, 5'-GCTGTTCTGGAGTAAGCTTGTGC-3'; miR-200a-3p-F, 5'-TAACACTGTCTGGTAACGATGT-3' and miR-200a-3p-R, 5'-CATCTTACCGGACAGTGCTGGA-3'; MAP3K2-F, 5'-TACACCCGTCAGATTCTGGAGG-3' and MAP3K2-R, 5'-ATGGTCTGAAGCCGTTTGC TGG-3'; GAPDH-F, 5'-TGCACCACCAACTGCTT AGC-3' and GAPDH-R, 5'-AGCTCAGGGATGACC TTGCC-3'; U6-F, 5'-CTCGCTTCGGCAGCACA-3' and U6-R, 5'-AACGCTTCACGAATTTGCGT-3'.

RNase R digestion and Actinomycin D treatment

Total RNA (5 μg) derived from Huh7-1.3 and HepG2.2.15 cells were treated with RNase R (Epicentre Biotechnologies, Shanghai, China) (RNase R+) or not (RNase R-) at 37°C for 0.5 h. The resulting RNA was subjected to qRT-PCR assay to detect the expression of circBACH1 and linear BACH1.

Actinomycin D treatment was also carried out to test the stability of circBACH1. 2 mg/mL actinomycin D (Cell Signaling Technology, Danvers, MA, USA) or dimethyl sulfoxide (DMSO) reagent (Cell Signaling Technology) was added into Medium of HepG2.2.15 and Huh7-1.3 cells and incubated for the indicated time (0 h, 4 h, 8 h, 12 h, 20 h or 24 h). Then, the levels of circBACH1 and linear BACH1 were assessed via qRT-PCR assay.

HBV replication detection

After transfection, enzyme-linked immunosorbent assay (ELISA) kits (Cell Biolabs, Inc., San Diego, CA, USA) were applied to examine the levels of HBV replication markers HBeAg (VPK-5003) and HBsAg (VPK-5004) in the supernatant of HepG2.2.15 and Huh7-1.3 cells as per the supplier's instructions.

For the determination of HBV DNA copy, qRT-PCR was implemented referring to a former report (Song et al., 2013). And HBV cccDNA was detected as previously reported (Tajik et al., 2015).

Cell viability assay

Cell Counting Kit-8 (CCK-8) assay was adopted to assess cell viability. After transfection, Huh7-1.3 and HepG2.2.15 cells were maintained in 96-well plates for the indicated time (0 h, 24 h, 48 h or 72 h), 10 μL CCK-8 solution (Sigma-Aldrich, St. Louis, MO, USA) was dropped into every well. After incubation for 2 h, the optical density (OD) at 450 nm was determined by exploiting a microplate reader (Molecular Devices, Sunnyvale, CA, USA).

Colony formation assay

1×10^3 transfected Huh7-1.3 and HepG2.2.15 cells were inoculated into 6-well plates and cultivated for 10 d. Colonies in each well were fastened using 4% paraformaldehyde (PFA; Sigma-Aldrich) and dyed with crystal violet (Sigma-Aldrich), then counted using Image J software (NIH, Bethesda, MD, USA) and photographed.

Cell metastasis assay

Transwell chambers (Costar, Corning, NY, USA) were applied for cell invasion examination. After transfection, 5×10^4 Huh7-1.3 and HepG2.2.15 cells were suspended in Medium without serum then transferred into upper chambers pre-enveloped with Matrigel (BD Bioscience, Franklin Lakes, NJ, USA). Meanwhile, complete Medium was added into lower chambers. At incubation for 24 h, cells remaining on the top side were washed away by phosphate buffer saline (PBS; Sigma-Aldrich), while invading cells were subjected to immobilization with 4% PFA (Sigma-Aldrich), dyed using crystal violet (Sigma-Aldrich), observed (100×) and counted under a microscope (Olympus, Tokyo, Japan).

Wound healing assay was carried out to evaluate the migratory capacity of HBV-transfected cells. Transfected Huh7-1.3 and HepG2.2.15 cells were placed into 24-well plates containing complete Medium until cell confluence reached 90%. Subsequently, scratches were made using sterile pipette tips (10 μL). Detached cells were removed by PBS (Sigma-Aldrich), then images were taken at 0 h and 24 h post-incubation at 37°C.

Flow cytometry

An Apoptosis Detection kit (BD Bioscience) was applied to analyze cell apoptosis referring to the user's manual. Transfected Huh7-1.3 and HepG2.2.15 cells were harvested and dyed with Annexin V-fluorescein isothiocyanate (FITC) and propidium iodide (PI) solution. Then apoptotic HBV-transfected cells were identified by a flow cytometer (BD Bioscience) and apoptosis rate was computed by the feat of Cell Quest 6.0 software (BD Bioscience).

Western blotting

Clinical specimens and cells were exposed to Radio-Immunoprecipitation Assay buffer (Cell Signaling Technology) to isolate total protein samples, followed by concentration quantification using a bicinchoninic acid protein assay kit (Sigma-Aldrich). Afterward, 40 μL protein samples were run on 12% sodium dodecyl sulfate (SDS)-polyacrylamide gels (PAGE), then transferred on polyvinylidene difluoride membranes (Millipore, Billerica, MA, USA). Later, membranes were blocked with blocking reagent (5% non-fat milk) and incubated rabbit primary antibody against Proliferating Cell Nuclear Antigen (PCNA; ab92552; Abcam, Cambridge, MA, USA), BCL2-Associated X (Bax;

ab182733; Abcam), B-cell lymphoma-2 (Bcl-2; ab237892; Abcam), MAP3K2 (ab33918; Abcam) or loading control GAPDH (ab181602; Abcam), then probed with goat anti-rabbit secondary antibody (ab205718; Abcam). In the end, protein bands were visualized and detected using enhanced chemiluminescence reagent (Cell Signaling Technology) and Image J software, respectively.

Dual-luciferase reporter assay (DLRA)

The target relationship in this study was forecast via Starbase 3.0 (http://starbase.sysu.edu.cn/). For DLRA, wide type luciferase reports of circBACH1 and MAP3K2 3'UTR (circBACH1 wt and MAP3K2 3'UTR wt) were built by inserting their partial sequence harboring the complementary position (5'-AGUGUU-3') with miR-200a-3p into pMirGLO reporter vector (Promega, Fitchburg, WI, USA), respectively. After mutating the complementary position (5'-UCACAA-3'), mutant reports (circBACH1 mut and MAP3K2 3'UTR mut) were constructed in a similar manner. 293T cells were co-transfected with luciferase report and mimic NC or miR-200a-3p mimic for 48 h. Luciferase density was determined by exploiting the Dual-Luciferase Reporter detection System (Promega) referring to the producer's guidance.

RNA immunoprecipitation (RIP) assay

This assay was performed with an EZ-Magna RIP Kit (Millipore) according to the supplier's guidelines. In brief, cell lysate of Huh7-1.3 and HepG2.2.15 cells were mixed with magnetic beads and antibodies against Argonaute2 (anti-Ago2; ab186733; Abcam) or immunoglobulin G (anti-IgG; ab133470; Abcam) on a shaker at 4°C overnight. Then, RNA was purified from magnetic beads-binding complexes after Proteinase K (Invitrogen) treatment. Finally, the enrichment of circBACH1, miR-200a-3p, and MAP3K2 was determined via qRT-PCR assay or Western blotting.

Xenograft model assay

The current experiment performed on nude mice was permitted by the Ethics Committees of Suizhou Central Hospital Affiliated to Hubei Medical College. Twelve BALB/c nude mice were commercially procured from Beijing Vital River Laboratory Animal Technology Co., Ltd. (Beijing, China) and supplemented with enough food and water. 2×10^6 HepG2.2.15 cells stably expressing small hairpin RNA (shRNA) targeting circBACH1 (sh-circBACH1) or its negative control sh-NC was hypodermically injected into nude mice (n=6). Subsequently, tumor growth was recorded every 5 days (Volume=width$^2\times$length/2). 30 days post-inoculation, all mice were euthanized and tumor tissues were resected. The levels of circBACH1, miR-200a-3p, and MAP3K2 were evaluated by qRT-PCR assay.

Statistical analysis

All data in this were derived from ≥3 independent experiments, processed via SPSS 20.0 software (SPSS, Chicago, IL, USA), then exhibited mean ± standard deviation. The difference in groups was determined by analysis of variance or Student's t-test. Correlation of circBACH1, miR-200a-3p, and MAP3K2 expression in 31 cases of HCC tissues was assessed via Pearson's correlation analysis. When $P<0.05$, it was considered statistically significant.

Results

CircBACH1 was highly expressed in HCC tissues and HBV-transfected hepatoma cells

At first, we examined the relative level of circBACH1 in HCC tissues. As illustrated in Fig. 1A, circBACH1 expression in HCC tissues was increased when compared to matched normal tissues. Additionally, circBACH1 expression was higher in Huh7-1.3 and HepG2.2.15 cells than that in their respective parent cells (Fig. 1B). CircBACH1 (ID: hsa_circ_0061395) is derived from exon 3-4 of the BACH1 gene located on chromosome 9 and its length is 1542 bp (Fig. 1C). After RNase R treatment, the level of linear BACH1 was obviously reduced in Huh7-1.3 and HepG2.2.15 cells, while circBACH1 expression was without change (Fig. 1D). Moreover, linear BACH1 was more likely to be degraded by actinomycin D, while circBACH1 was more resistant to actinomycin D in Huh7-1.3 and HepG2.2.15 cells (Fig. 1E). The above results suggested that circBACH1 might be associated with hepatoma development.

CircBACH1 knockdown was able to repress HBV replication and proliferation in HBV-transfected hepatoma cells

The dysregulation of circBACH1 in HCC tissues and HBV-transfected hepatoma cells prompted us to investigate the influence of circBACH1 on hepatoma progression. Then Huh7-1.3 and HepG2.2.15 cells with circBACH1 deficiency were established by transfection with special small interfering RNAs of circBACH1. As exhibited in Fig. 2A, the introduction of si-circBACH1#1, si-circBACH1#2 or si-circBACH1#3 successfully decreased circBACH1 expression in Huh7-1.3 and HepG2.2.15 cells, with si-NC as a negative control. Furthermore, si-circBACH1#2 triggered the best knockdown effect, so it was selected for later assays. We found that circBACH1 knockdown reduced the levels of HBeAg and HBsAg in HBV-transfected hepatoma cells (Fig. 2B,C). And depletion of circBACH1 decreased HBV DNA copies (Fig. 2D) and HBV cccDNA (Fig. 2E)

in Huh7-1.3 and HepG2.2.15 cells. CCK-8 assay disclosed that silencing of circBACH1 repressed cell viability of Huh7-1.3 and HepG2.2.15 cells (Fig. 2F). And depletion of circBACH1 reduced clonogenicity of Huh7-1.3 and HepG2.2.15 cells, which was uncovered via colony formation assay (Fig. 2G). These data collectively suggested that silencing of circBACH1 was able to hinder HBV replication and proliferation in HBV-transfected hepatoma cells.

Depression of circBACH1 was able to restrain metastasis and induce apoptosis in HBV-transfected hepatoma cells

Furthermore, we further assessed the effects of circBACH1 silencing on metastasis and apoptosis rate in HBV-transfected hepatoma cells. As shown in Fig. 3A,B, Transwell assay and Wound healing assay proved that circBACH1 knockdown was able to suppress cell invasion and migration of Huh7-1.3 and HepG2.2.15 cells. In addition, a higher apoptotic rate was detected in Huh7-1.3 and HepG2.2.15 cells of si-circBACH1#2 group compared to that in cells of the si-NC group (Fig. 3C). Moreover, circBACH1 depletion reduced the levels of PCDA and Bcl-2, and increased Bax level in Huh7-1.3 and HepG2.2.15 cells (Fig. 3D). These data collectively suggested that silencing of circBACH1 suppressed HBV replication, proliferation, and metastasis in HBV-transfected hepatoma cells.

CircBACH1 was able to sponge miR-200a-3p

To clarify the mechanism by which circBACH1 altered the cellular behaviors of HBV-transfected hepatoma cells, Starbase 3.0 was searched to predict the miRNAs potentially interacting with circBACH1, and miR-200a-3p was discovered to be a candidate. The binding sites between the two are exhibited in Fig. 4A. The following dual-luciferase reporter assay revealed that overexpression of miR-200a-3p efficiently reduced

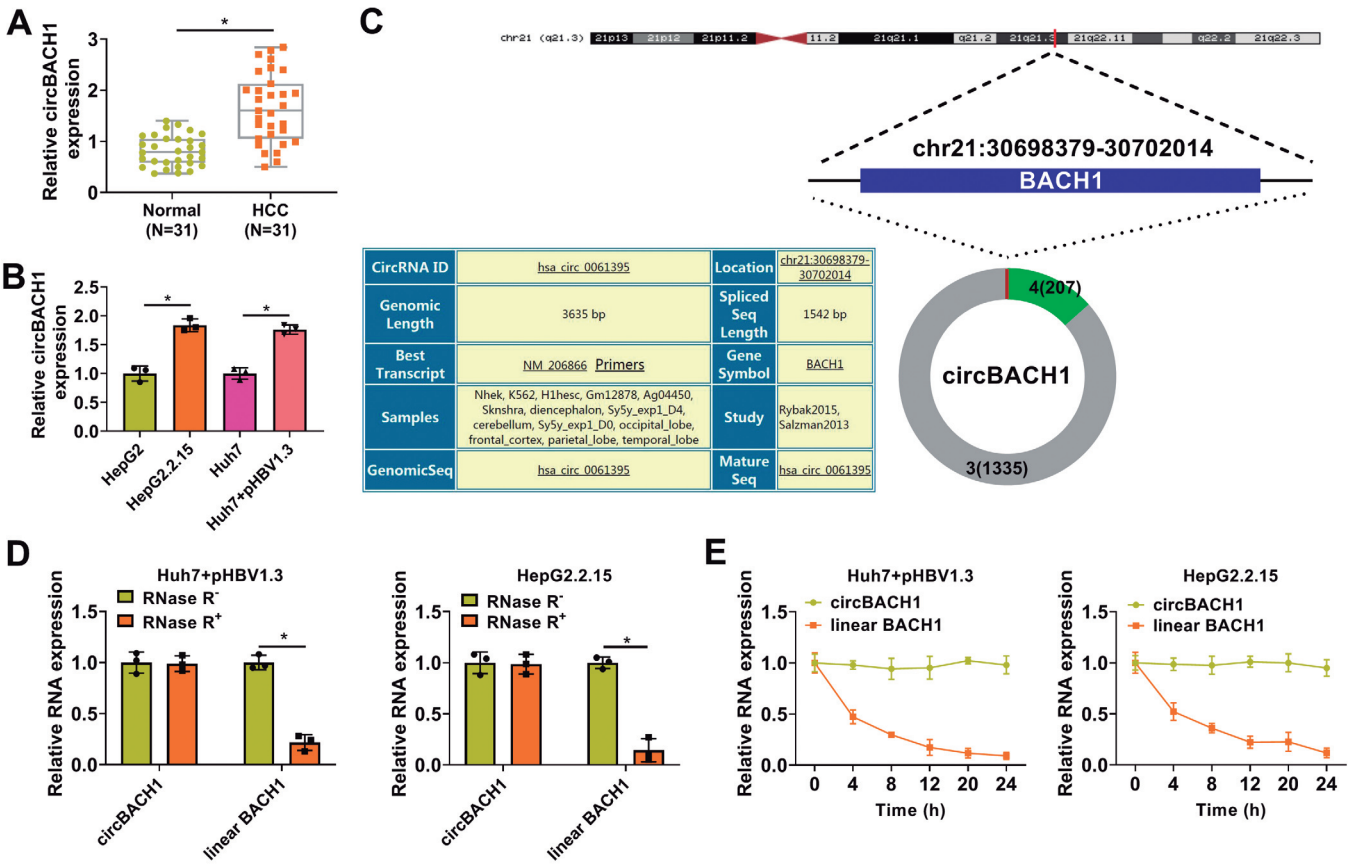

Fig. 1. CircBACH1 was highly expressed in HCC tissues and HBV-transfected hepatoma cells. **A.** QRT-PCR assay for the relative expression of circBACH1 in HCC tissues and normal tissues (N=31). **B.** QRT-PCR assay for the relative expression of circBACH1 in HepG2, HepG2.2.15, Huh7, and Huh7-1.3 cells. **C.** Schematic diagram of the structure and other information of circBACH1. **D.** QRT-PCR assay for the relative expression of circBACH1 and linear BACH1 in RNA isolated from Huh7-1.3 and HepG2.2.15 cells digested with RNase R (RNase R+) or not (RNase R-). **E.** QRT-PCR assay for the half-life of circBACH1 and linear BACH1 in Huh7-1.3 and HepG2.2.15 cells incubated with DMSO or actinomycin D. *P<0.05.

the luciferase activity of 293T cells co-transfected with circBACH1 wt, while it did not alter that of cells co-transfected with circBACH1 mut (Fig. 4B). To further consolidate the binding between circBACH1 and miR-200a-3p, RIP assay showed that both circBACH1 and miR-200a-3p could be immunoprecipitated by anti-Ago2 (Fig. 4C). Furthermore, miR-200a-3p expression was observed to be decreased in HCC tissues and HBV-transfected hepatoma cells relative to corresponding control (Fig. 4D,E). There existed an inverse correlation between the expression levels of circBACH1 and miR-200a-3p in HCC tissues (Fig. 4F). Therefore, circBACH1 directly binds to miR-200a-3p.

Silencing of circBACH1 suppressed the progression of hepatoma cells by sponging miR-200a-3p

We then explored the association between miR-200a-3p and circBACH1 in HBV replication and hepatoma development. QRT-PCR assay uncovered the knockdown efficiency of miR-200a-3p inhibitor in reducing miR-200a-3p expression in Huh7-1.3 and HepG2.2.15 cells, with respect to inhibitor NC (Fig. 5A). Moreover, depletion of circBACH1 apparently increased miR-200a-3p level in HBV-transfected hepatoma cells, while miR-200a-3p inhibitor attenuated it (Fig. 5B). Consequent functional assays were performed and indicated that circBACH1 knockdown-induced the decreased levels of HBeAg (Fig. 5C) and HBsAg (Fig. 5D), HBV DNA copies (Fig. 5E) and HBV cccDNA (Fig. 5F), the inhibited cell viability (Fig. 5G), colony formation ability (Fig. 5H), invasion (Fig. 5I) and migration (Fig. 5J). The elevated apoptotic rate (Fig. 5K), as well as the reduced PCDA and Bcl-2 levels and enhanced Bax level (Fig. 5L) in Huh7-1.3 and HepG2.2.15 cells were all largely relieved by miR-200a-3p inhibition. Hence, silencing of circBACH1 hampered HBV replication, proliferation, and metastasis in HBV-transfected hepatoma cells by increasing miR-200a-3p expression.

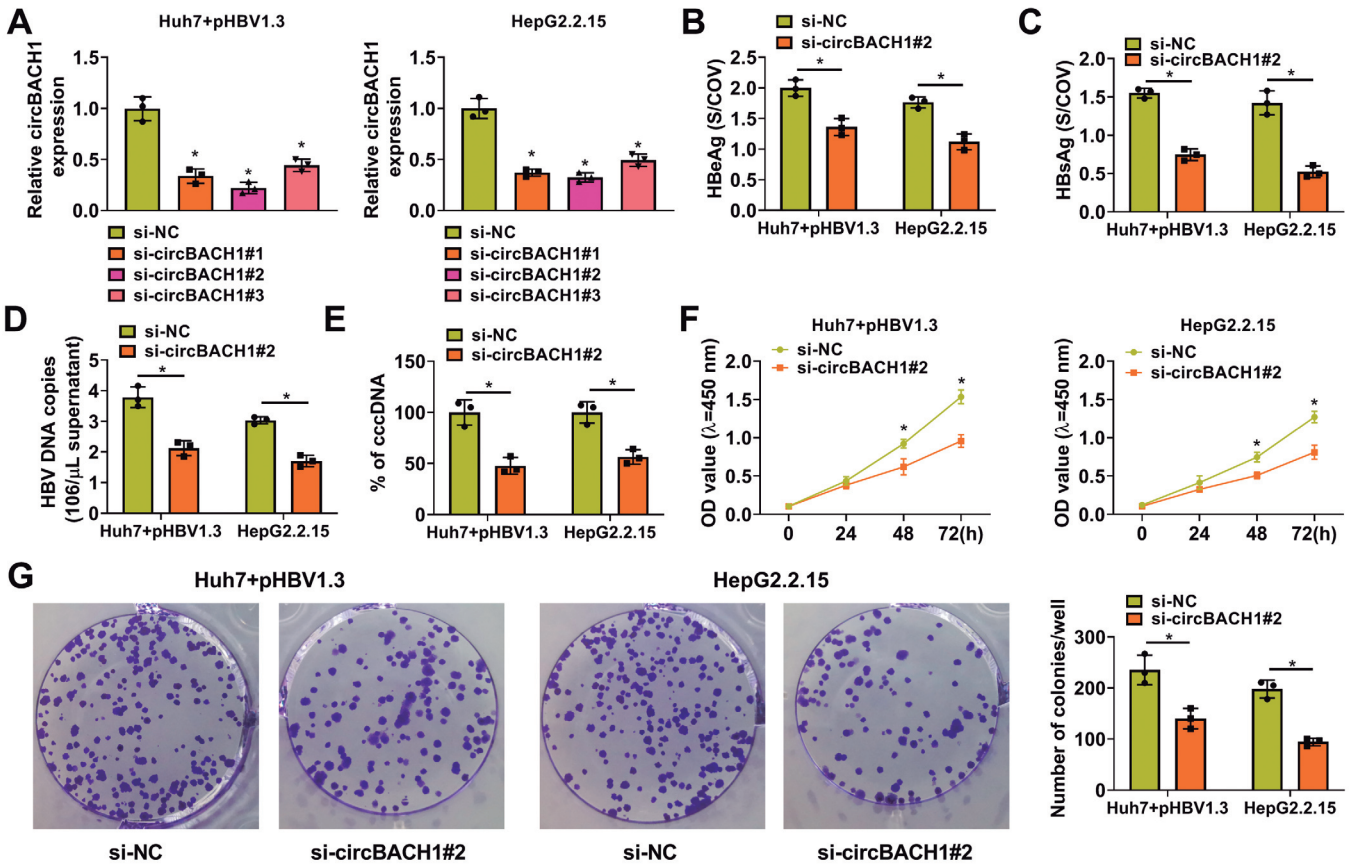

Fig. 2. CircBACH1 knockdown inhibited HBV replication and proliferation in HBV-transfected hepatoma cells. **A.** QRT-PCR assay for the relative expression of circBACH1 in Huh7-1.3 and HepG2.2.15 cells transfected with si-NC, si-circBACH1#1, si-circBACH1#2 or si-circBACH1#3. **B-G.** Huh7-1.3 and HepG2.2.15 cells were transfected with si-NC or si-circBACH1#2. **B, C.** ELISA assay for the levels of HBeAg **(B)** and HBsAg **(C)** in transfected cells. **D, E.** QRT-PCR assay for HBV DNA copies **(D)** and HBV cccDNA **(E)** in transfected cells. **F.** CCK-8 assay for the cell viability of transfected cells. **G.** Colony formation assay for the cell clonogenicity of transfected cells. *P<0.05.

MAP3K2 acted as a downstream gene of circBACH1/miR-200a-3p axis

To search the downstream effector of circBACH1/miR-200a-3p axis, Starbase 3.0 was used to predict the target gene of miR-200a-3p. 3'UTR of MAP3K2 was discovered to be endowed with the complementary sequence with miR-200a-3p (Fig. 6A). Dual-luciferase reporter assay suggested that enforced expression of miR-200a-3p obviously decreased the

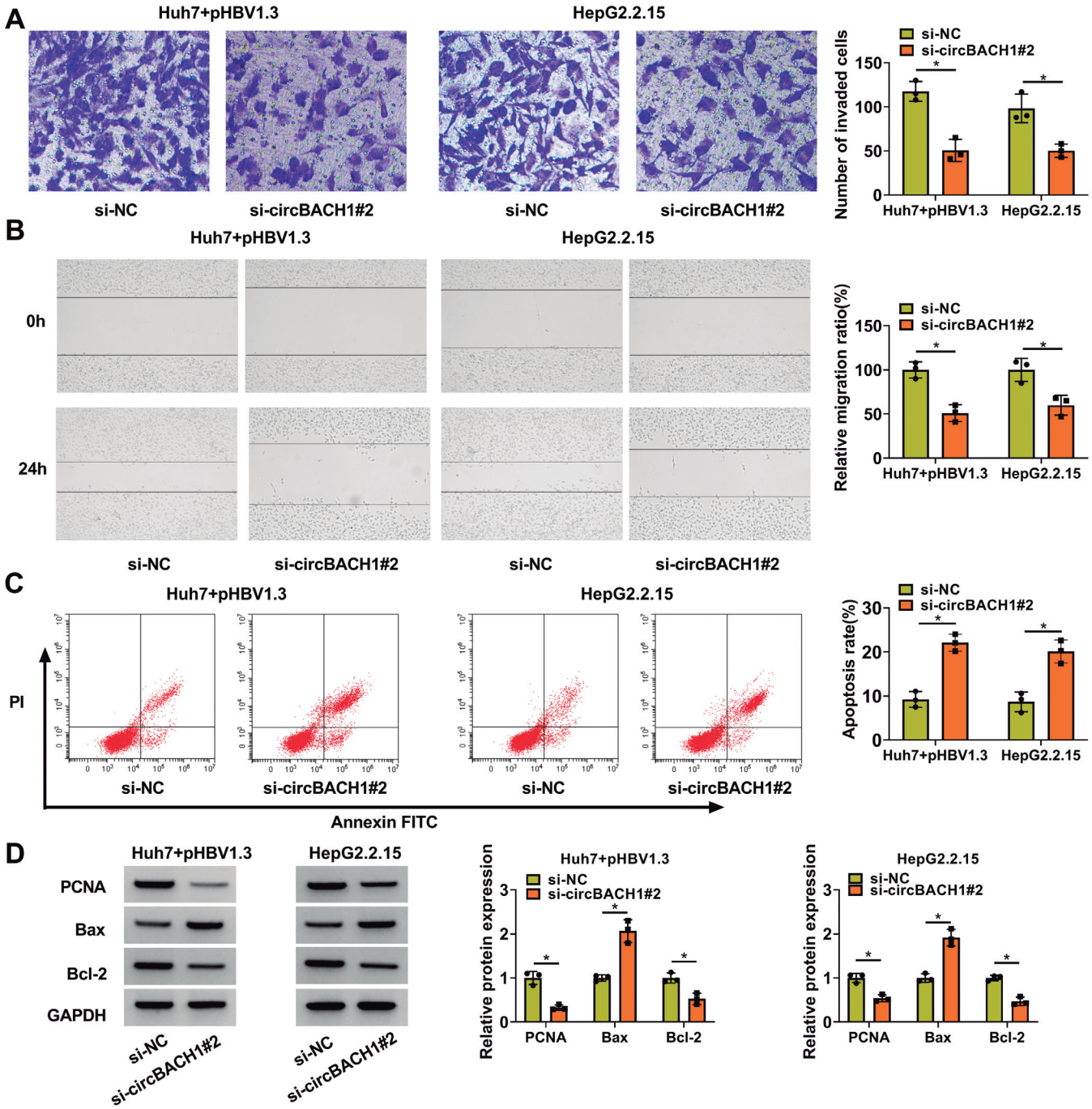

Fig. 3. CircBACH1 deficiency was able to suppress metastasis and induce apoptosis in HBV-transfected hepatoma cells. **A-D.** Huh7-1.3 and HepG2.2.15 cells were transfected with si-NC or si-circBACH1#2. **A.** Transwell assay for the cell invasion in transfected cells. **B.** Wound healing assay for the cell migration in transfected cells. **C.** Flow cytometry for the apoptotic rate in transfected cells. **D.** Western blotting for the protein levels of PCNA, Bax, and Bcl-2 in transfected cells. *P<0.05.

luciferase activity of 293T cells co-transfected with MAP3K2 3'UTR wt, while the luciferase density of cells co-transfected with MAP3K2 3'UTR mut was without change (Fig. 6B). The consequent RIP assay also manifested the target relationship between miR-200a-3p and MAP3K2 (Fig. 6C). MAP3K2 expression was detected to be higher in HCC tissues than that in normal tissues (Fig. 6D,E). Likewise, the protein level of MAP3K2 was upregulated in HepG2.2.15 and Huh7-1.3 cells in contrast to HepG2 and Huh7 cells, respectively (Fig. 6F). Furthermore, miR-200a-3p expression in HCC tissues was negatively correlated with MAP3K2 mRNA expression (Fig. 6G). And MAP3K2 protein level in HepG2.2.15 and Huh7-1.3 cells was inhibited by circBACH1 depletion, which was remitted by miR-200a-3p inhibitor (Fig. 6H). Collectively, miR-200a-3p was able to target MAP3K2.

miR-200a-3p upregulation was able to suppress the development of hepatoma by targeting MAP3K2

We then investigated the co-effect of miR-200a-3p

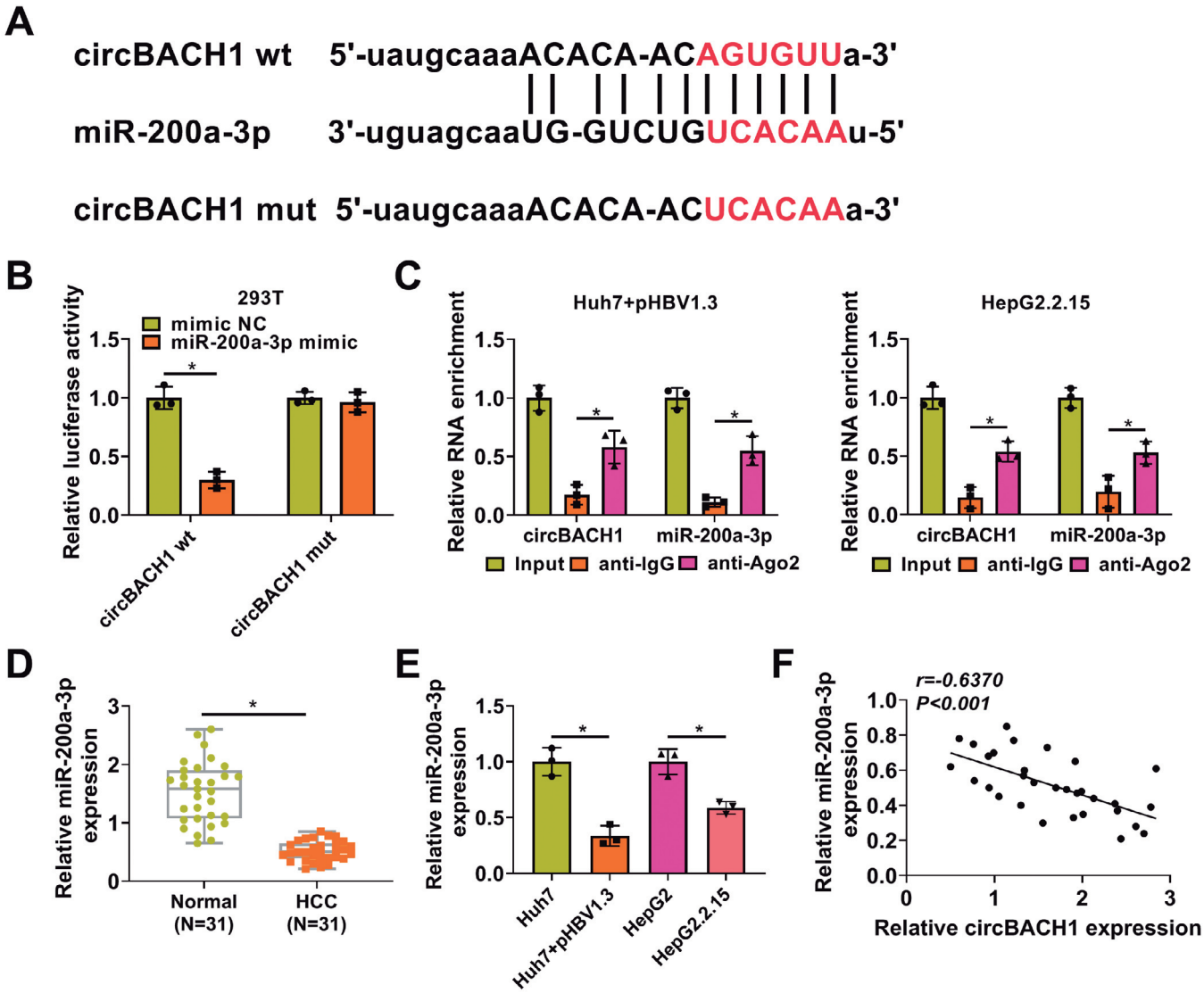

Fig. 4. CircBACH1 was able to sponge miR-200a-3p. **A.** The potential binding sites between circBACH1 and miR-200a-3p are predicted by Starbase 3.0. **B.** Dual-luciferase reporter assay for the luciferase activity of 293T cells co-transfected with mimic NC or miR-200a-3p mimic and circBACH1 wt or circBACH1 mut. **C.** RIP and qRT-PCR assays for the binding potency between circBACH1 and miR-200a-3p to Ago2 protein in Huh7-1.3 and HepG2.2.15 cells. **D.** QRT-PCR assay for the relative expression of miR-200a-3p in HCC tissues and normal tissues (N=31). **E.** QRT-PCR assay for the relative expression of miR-200a-3p in HepG2, HepG2.2.15, Huh7, and Huh7-1.3 cells. **F.** Pearson's correlation analysis for the correlation between the expression levels of circBACH1 and miR-200a-3p in 31 HCC tissues. *P<0.05.

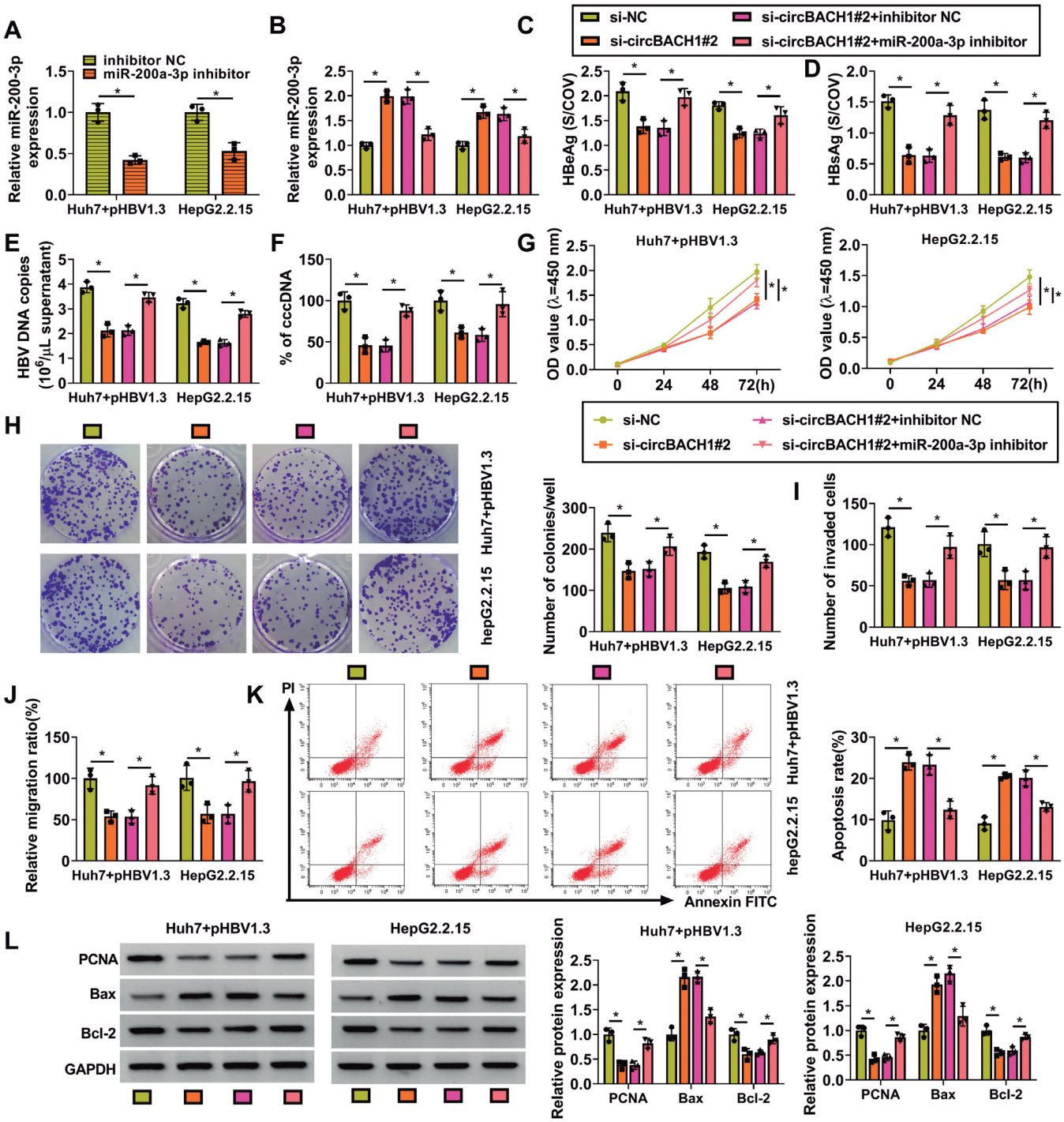

Fig. 5. CircBACH1 directly binds to miR-200a-3p to function in hepatoma cells. **A.** QRT-PCR assay for the relative expression of miR-200a-3p in Huh7-1.3 and HepG2.2.15 cells transfected with inhibitor NC or miR-200a-3p inhibitor. **B-M.** Huh7-1.3 and HepG2.2.15 cells were transfected with si-NC, si-circBACH1#2, si-circBACH1#2+inhibitor NC or si-circBACH1#2+miR-200a-3p inhibitor. **B.** QRT-PCR assay for the relative expression of miR-200a-3p in transfected cells. **C, D.** ELISA assay for the levels of HBeAg **(C)** and HBsAg **(D)** in transfected cells. (E-F) QRT-PCR assay for HBV DNA copies **(E)** and HBV cccDNA **(F)** in transfected cells. **G.** CCK-8 assay for the cell viability of transfected cells. **H.** Colony formation assay for the cell clonogenicity of transfected cells. **I.** Transwell assay for the cell invasion in transfected cells. **J.** Wound healing assay for the cell migration in transfected cells. **K.** Flow cytometry for the apoptotic rate in transfected cells. **L.** Western blotting for the protein levels of PCNA, Bax, and Bcl-2 in transfected cells. *P<0.05.

and MAP3K2 on HBV replication and hepatoma development. As shown in Fig. 7A, transfection with miR-200a-3p mimic remarkably enhanced miR-200a-3p expression in Huh7-1.3 and HepG2.2.15 cells, relative to mimic NC. And Huh7-1.3 and HepG2.2.15 cells with MAP3K2 overexpression were established by introduction with pcDNA-MAP3K2, with pcDNA as negative control (Fig. 7B). Subsequently, our data exhibited that the overexpression of MAP3K2 obviously abolished the inhibitory effect of miR-200a-3p mimic on HBeAg (Fig. 7C) and HBsAg (Fig. 7D) levels, HBV DNA copies (Fig. 7E), and HBV cccDNA (Fig. 7F) in Huh7-1.3 and HepG2.2.15 cells. Meanwhile, functional analysis discovered that the upregulation of miR-200a-3p was able to suppress cell viability (Fig. 7G), colony formation ability (Fig. 7H), invasion (Fig. 7I), migration (Fig. 7J), and induce apoptotic rate (Fig. 7K), which was partly overturned by the introduction of pcDNA-MAP3K2 in Huh7-1.3 and HepG2.2.15 cells. Also, the changes of PCDA, Bcl-2, and Bax protein levels (Fig. 7L) under the same condition further verified the effects of miR-200a-3p and MAP3K2 on proliferation and apoptosis of Huh7-1.3 and HepG2.2.15 cells. Taken together, miR-200a-3p impeded HBV replication and hepatoma development by directly targeting MAP3K2.

CircBACH1 exerted a tumor-promoting role in hepatoma in vivo

A xenograft mouse model was established to evaluate the impact of circBACH1 on hepatoma growth *in vivo*. Smaller volumes (Fig. 8A) and lighter weight

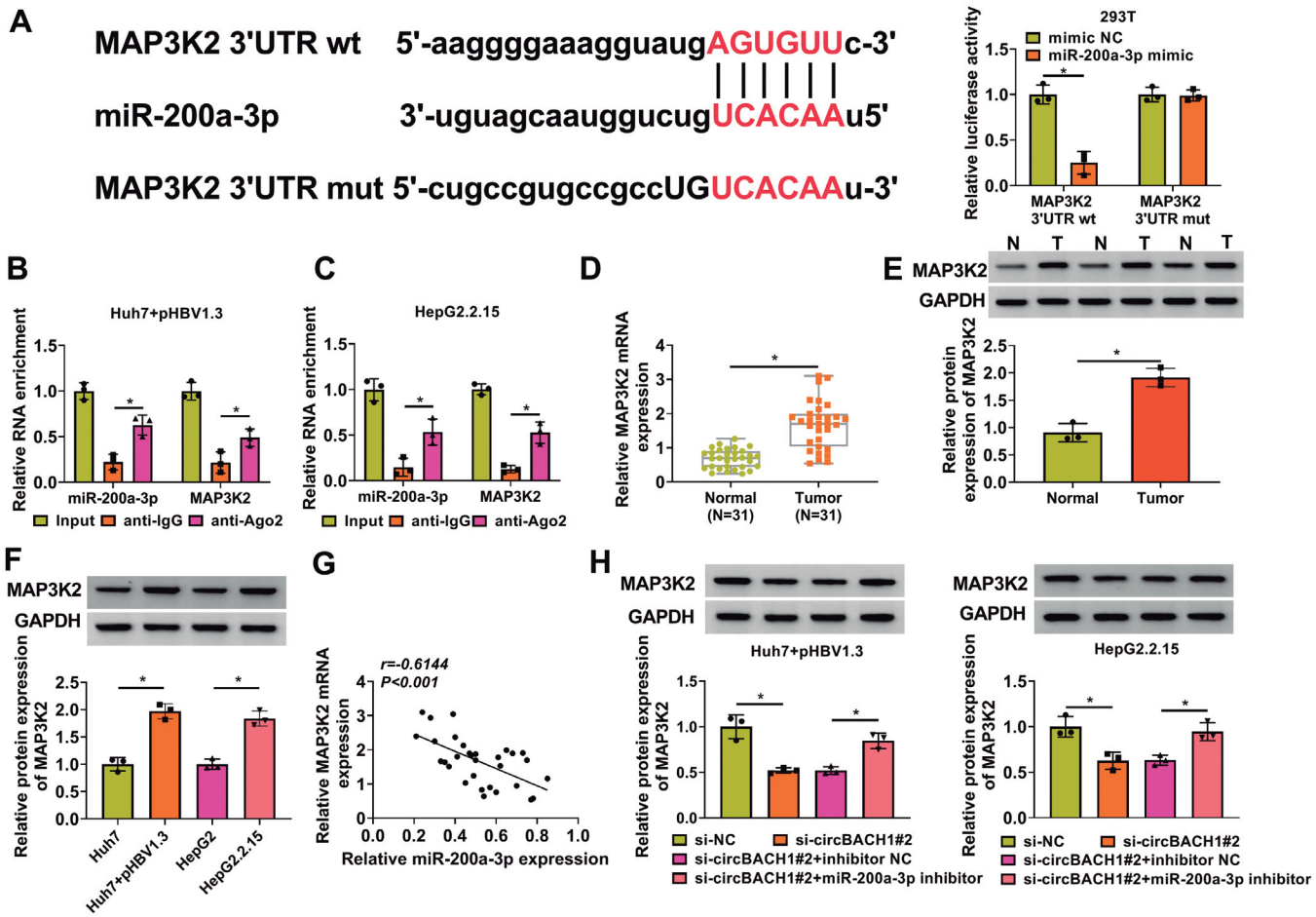

Fig. 6. MAP3K2 as a downstream gene of circBACH1/miR-200a-3p axis. **A.** The potential binding sites between miR-200a-3p and MAP3K2 3'UTR are forecast by Starbase 3.0. **B.** Dual-luciferase reporter assay for the luciferase activity of 293T cells co-transfected with mimic NC or miR-200a-3p mimic and MAP3K2 3'UTR wt or MAP3K2 3'UTR mut. **C.** RIP and qRT-PCR assays for the binding potency between circBACH1 and miR-200a-3p. **D.** QRT-PCR assay for the relative mRNA expression of MAP3K2 in HCC tissues and normal tissues (N=31). **E.** Western blotting for the protein level of MAP3K2 in HCC tissues and normal tissues. **F.** Western blotting for the protein level of MAP3K2 in HepG2, HepG2.2.15, Huh7, and Huh7-1.3 cells. **G.** Pearson's correlation analysis for the correlation between the expression levels of miR-200a-3p and MAP3K2 mRNA in 31 HCC tissues. **H.** Western blotting for the protein level of MAP3K2 in Huh7-1.3 and HepG2.2.15 cells transfected with si-NC, si-circBACH1#2, si-circBACH1#2+inhibitor NC or si-circBACH1#2+miR-200a-3p inhibitor. *P<0.05.

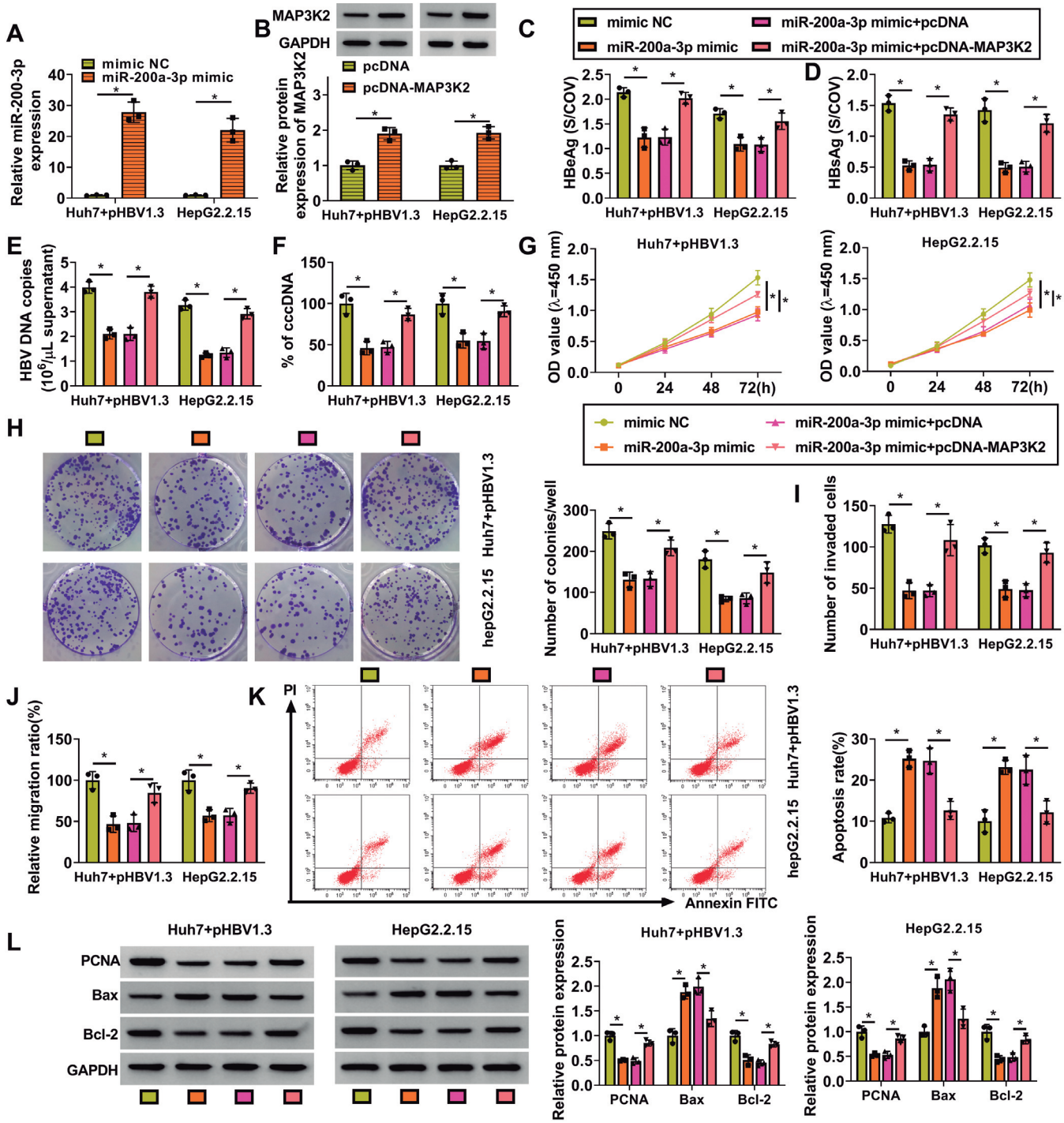

Fig. 7. Gain of miR-200a-3p was able to suppress HBV replication, proliferation, and metastasis in HBV-transfected hepatoma cells by targeting MAP3K2. **A.** QRT-PCR assay for the relative expression of miR-200a-3p in Huh7-1.3 and HepG2.2.15 cells transfected with mimic NC or miR-200a-3p mimic. **B.** Western blotting for the protein level of MAP3K2 in Huh7-1.3 and HepG2.2.15 cells transfected with pcDNA or pcDNA-MAP3K2. **C-L.** Huh7-1.3 and HepG2.2.15 cells were transfected with mimic NC, miR-200a-3p mimic, miR-200a-3p mimic+pcDNA or miR-200a-3p mimic+pcDNA-MAP3K2. **C, D.** ELISA assay for the levels of HBeAg **(C)** and HBsAg **(D)** in transfected cells. **E, F.** QRT-PCR assay for HBV DNA copies **(E)** and HBV cccDNA **(F)** in transfected cells. **G.** CCK-8 assay for the cell viability of transfected cells. **H.** Colony formation assay for the cell clonogenicity of transfected cells. **I.** Transwell assay for the cell invasion in transfected cells. **J.** Wound healing assay for the cell migration in transfected cells. **K.** Flow cytometry for the apoptotic rate in transfected cells. **L.** Western blotting for the protein levels of PCNA, Bax, and Bcl-2 in transfected cells. *P<0.05.

(Fig. 8B) were detected in mice of the sh-circBACH1 group in contrast to the sh-NC group. QRT-PCR assay and Western blotting were employed to examine the levels of circBACH1, miR-200a-3p and MAP3K2 in the xenografts. The expression of circBACH1 and MAP3K2 was decreased, while miR-200a-3p was increased in the tumor from the sh-circBACH1 group relative to the -NC group (Fig. 8C,D). In sum, circBACH1 acted as an oncogenic circRNA in hepatoma progression.

Discussion

Chronic HBV infection is evidenced to be a crucial causal factor of primary liver cancers, including HCC (Tharayil and Roberts, 2006; Neuveut et al., 2010). Many dysregulated circRNAs are implicated with the occurrence and progression of HBV-related HCC (Cui et al., 2018). In this work, we identified an upregulated circRNA, circBACH1, in HCC tissues and HBV-transfected hepatoma cells. And we manifested its cancerogenic role in hepatoma development.

Benefiting from high-throughput RNA sequencing and bioinformatic analysis methods, increasing functional circRNAs have been discovered (Huang et al., 2017). Accumulating works suggested that certain circRNAs were involved in HBV-related live diseases. For example, circRNA_101764 was lowly expressed in HBV-related hepatoma and it might play important role in hepatoma (Wang et al., 2018). Plasma circPanel might be applied for the diagnosis of HBV-related HCC (Yu et al., 2020). In addition, circRNA_10156 was testified to have a pro-tumorigenic function in HBV-associated hepatoma (Wang et al., 2020). Liu et al. corroborated that circBACH1 expression was highly enriched in HCC tissues and cells, and it was able to contribute to HCC cell growth (Liu et al., 2020). Here, our data also uncovered the upregulation of circBACH1 in HCC tissues, as well as the HBV-transfected hepatoma cells.

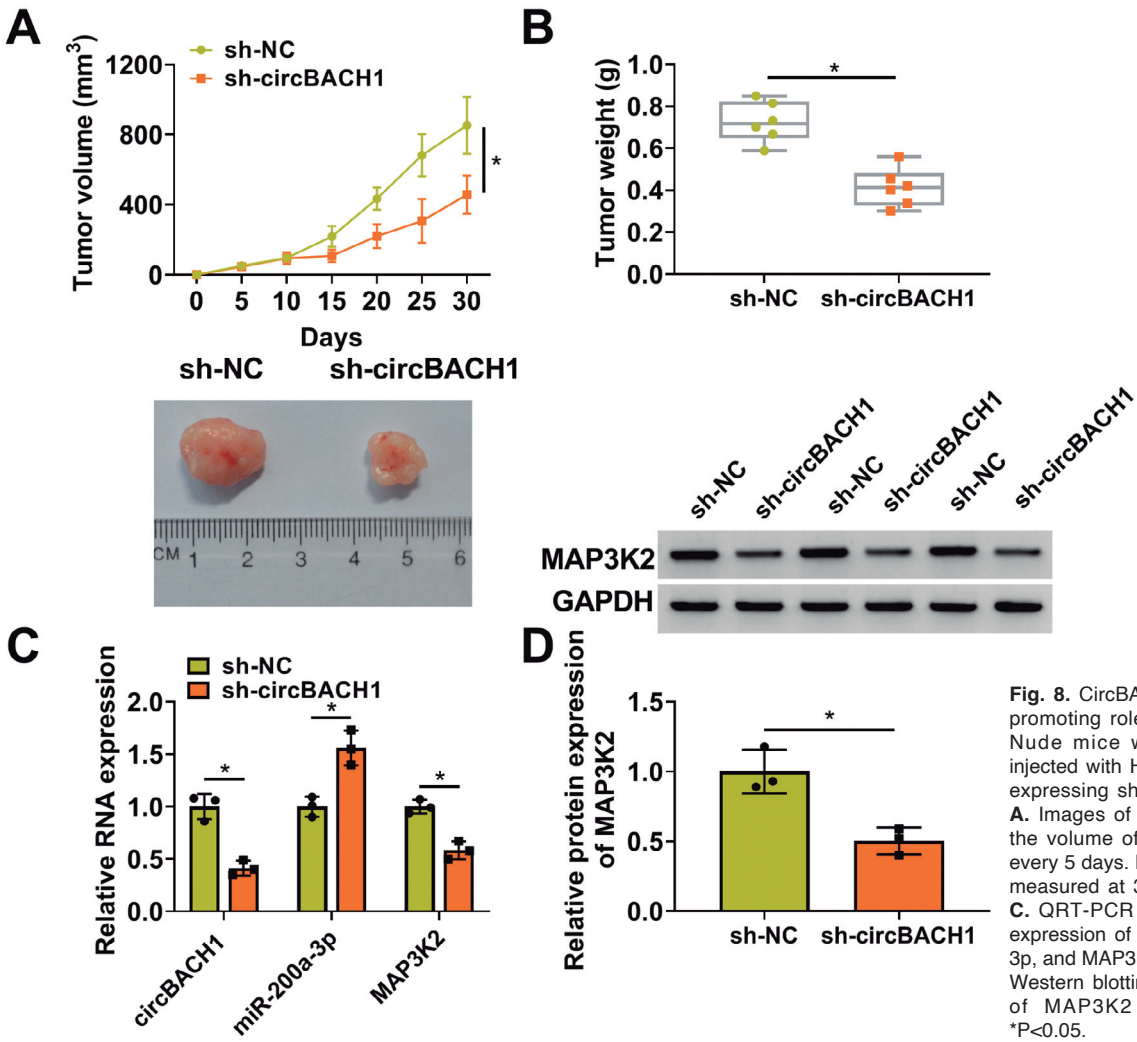

Fig. 8. CircBACH1 exerted a tumor-promoting role in hepatoma *in vivo*. Nude mice were hypodermically injected with HepG2.2.15 cells stably expressing sh-NC or sh-circBACH1. **A.** Images of xenografts, as well as the volume of xenografts measured every 5 days. **B.** Weight of xenografts measured at 30 days after injection. **C.** QRT-PCR assay for the relative expression of circBACH1, miR-200a-3p, and MAP3K2 in the xenografts. **D.** Western blotting for the protein level of MAP3K2 in the xenografts. *P<0.05.

Besides, HBV replication has been reported to be the primary driving force for HBV-related diseases, so inhibition or elimination of HBV replication is thought to reduce the risk of or slow the progression of these diseases (Liaw, 2013). It has been confirmed that HBsAg is a hallmark of HBV infection, and HBeAg represents the activity of HBV replication (Kao, 2008). In this paper, our data exhibited that circBACH1 knockdown was able to obviously repress the levels of HBeAg and HBsAg in HBV-transfected hepatoma cells. Hence, we speculated that circBACH1 might exert functions in HBV-related hepatoma. Loss-of-function assays demonstrated that circBACH1 knockdown suppressed HBV replication, growth, and metastasis in HBV-transfected hepatoma cells, indicating the oncogenic role of circBACH1 in HBV-associated hepatoma.

It is widely accepted that the regulatory efficacy of circRNAs is principally attributed to their miRNA sponge competence (Kulcheski et al., 2016). In this study, miR-200a-3p was confirmed to be a target miRNA of circBACH1. As a tumor suppressor, miR-200a-3p was documented in gastric cancer (Jia et al., 2019), renal carcinoma (Ding et al., 2018), and HCC (Gong et al., 2018). Inversely, miR-200a-3p was also reported to be a tumor-promoting factor in ovarian cancer (Shi et al., 2019) and esophageal cancer (Zang et al., 2016). The expression of miR-200a-3p was decreased in cancerous liver tissues, and it could be a promising biomarker for HCC diagnosis and prognosis (Tak et al., 2018). As previously described, miR-200a-3p was downregulated in HBV-positive tissues and cells, and it had an inhibitory role in the proliferation and metastasis of HBV-positive cells (Shi et al., 2017). Consistent with this former report, our data showed that the miR-200a-3p level was reduced in HCC tissues and HBV-transfected hepatoma cells. Likewise, HBV replication, growth, and metastasis were inhibited in HBV-transfected hepatoma cells with miR-200a-3p overexpression. Moreover, miR-200a-3p silencing attenuated circBACH1 deficiency-mediated the inhibited HBV replication, growth, and metastasis in HBV-transfected hepatoma cells. To conclude, circBACH1 positively modulated HBV replication, growth, and metastasis in HBV-transfected hepatoma cells by sponging miR-200a-3p.

MicroRNAs were tightly associated with HBV infection and HBV-associated hepatocarcinogenesis, which were potential HCC diagnosis markers and therapeutic targets (Xie et al., 2014). The establishment of a circRNA-miRNA-mRNA network might be helpful to lucubrate the mechanisms of hepatocarcinogenesis (Xiong et al., 2018). MAP3K2 was verified to be a downstream gene of miR-200a-3p. MAP3K2 was upregulated in HCC samples, which was responsible for the anti-tumor role of miR-1208 and miR-302a in HCC (Wang et al., 2019; Zhang et al., 2021). Furthermore, MAP3K2 in serum of patients infected with HBV was positively correlated with HBV-DNA copies (Chen et al., 2019a). Meanwhile, a previous study reported that the knockdown of MAP2K3 in poly(I-C) stimulated hepatocytes could lead to interferon-beta promoter activation (Kanda et al., 2021), suggesting the vital role

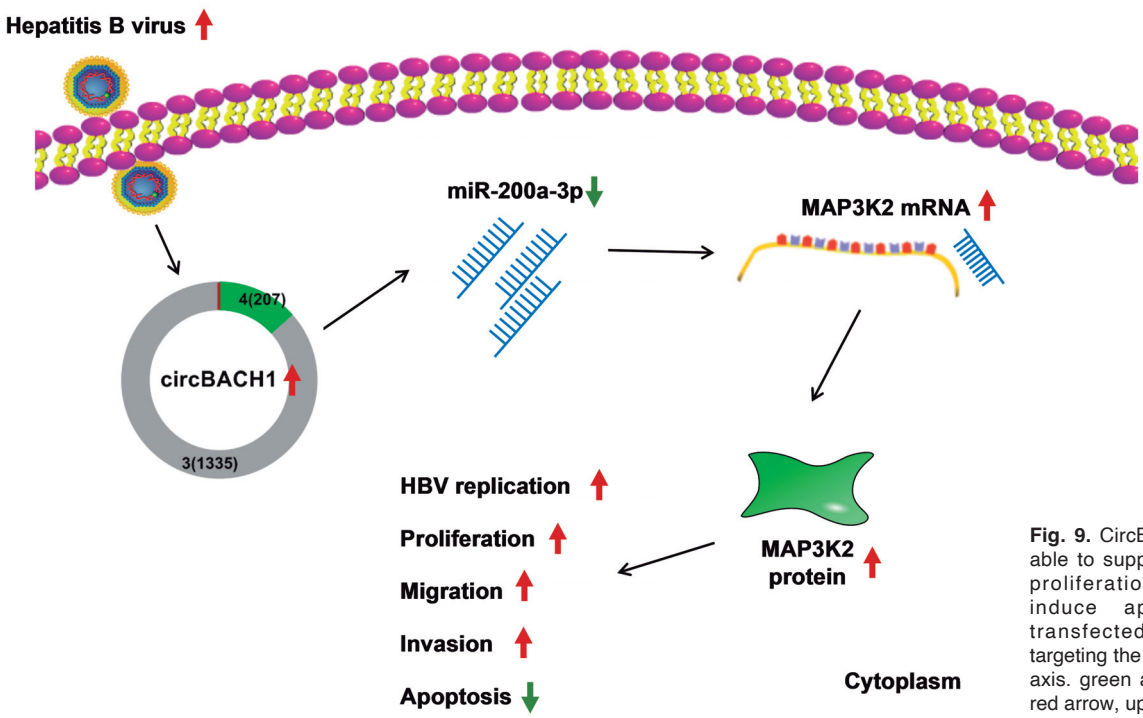

Fig. 9. CircBACH1 deficiency was able to suppress HBV replication, proliferation, metastasis, and induce apoptosis in HBV-transfected hepatoma cells by targeting the miR-200a-3p/MAP3K2 axis. green arrow, downregulation; red arrow, upregulation.

in antiviral immunity against HAV infection. Here, the expression level of MAP3K2 was verified to be increased in HCC tissues and HBV-transfected hepatoma cells. Our data also presented that the overexpression of MAP3K2 partly abolished the suppression role of miR-200a-3pon HBV replication, growth, and metastasis in HBV-transfected hepatoma cells. The above results revealed the involvement of circBACH1/miR-200a-3p/MAP3K2 axis in HBV replication and HBV-related hepatoma.

In summary, circBACH1 was highly expressed in HCC tissues and HBV-transfected hepatoma cells. CircBACH1 was able to facilitate HBV replication and aggravate HBV-associated hepatoma through the miR-200a-3p/MAP3K2 pathway (Fig. 9), implying that circBACH1 might be a potential therapeutic target for HBV-related hepatoma.

Disclosure of interest. The authors declare that they have no conflicts of interest.

References

Balogh J., Victor D., 3rd, Asham E.H., Burroughs S.G., Boktour M., Saharia A., Li X., Ghobrial R.M. and Monsour H.P. Jr (2016). Hepatocellular carcinoma: a review. J. Hepatocell. Carcinoma 3, 41-53.

Chen L.L. (2016). The biogenesis and emerging roles of circular RNAs. Nat. Rev. Mol. Cell Biol. 17, 205-211.

Chen S., Yang L., Pan A., Duan S., Li M., Li P., Huang J., Gao X., Huang X. and Lin Y. (2019a). Inhibitory effect on the hepatitis B cells through the regulation of miR-122-MAP3K2 signal pathway. An. Acad. Bras. Cienc. 91, e20180941.

Chen X., Gao J., Yu Y., Zhao Z. and Pan Y. (2019b). LncRNA FOXD3-AS1 promotes proliferation, invasion and migration of cutaneous malignant melanoma via regulating miR-325/MAP3K2. Biomed. Pharmacother. 120, 109438.

Cui S., Qian Z., Chen Y., Li L., Li P. and Ding H. (2018). Screening of up- and downregulation of circRNAs in HBV-related hepatocellular carcinoma by microarray. Oncol. Lett. 15, 423-432.

Ding M., Sun X., Zhong J., Zhang C., Tian Y., Ge J., Zhang C.Y., Zen K., Wang J.J., Zhang C. and Wang C. (2018). Decreased miR-200a-3p is a key regulator of renal carcinoma growth and migration by directly targeting CBL. J. Cell Biochem. 119, 9974-9985.

Fares N. and Peron J.M. (2013). Epidemiology, natural history, and risk factors of hepatocellular carcinoma. Rev. Prat. 63, 216-217, 220-212 (in French).

Gong Y., Mao J., Wu D., Wang X., Li L., Zhu L. and Song R. (2018). Circ-ZEB1.33 promotes the proliferation of human HCC by sponging miR-200a-3p and upregulating CDK6. Cancer Cell Int. 18, 116.

Huang J., Wang Y., Guo Y. and Sun S. (2010). Down-regulated microRNA-152 induces aberrant DNA methylation in hepatitis B virus-related hepatocellular carcinoma by targeting DNA methyltransferase 1. Hepatology 52, 60-70.

Huang T., She K., Peng G., Wang W., Huang J., Li J., Wang Z. and He J. (2016). MicroRNA-186 suppresses cell proliferation and metastasis through targeting MAP3K2 in non-small cell lung cancer. Int. J. Oncol. 49, 1437-1444.

Huang S., Yang B., Chen B.J., Bliim N., Ueberham U., Arendt T. and Janitz M. (2017). The emerging role of circular RNAs in transcriptome regulation. Genomics 109, 401-407.

Jia C., Zhang Y., Xie Y., Ren Y., Zhang H., Zhou Y., Gao N., Ding S. and Han S. (2019). miR-200a-3p plays tumor suppressor roles in gastric cancer cells by targeting KLF12. Artif. Cells Nanomed. Biotechnol. 47, 3697-3703.

Jiang R., Deng L., Zhao L., Li X., Zhang F., Xia Y., Gao Y., Wang X. and Sun B. (2011). miR-22 promotes HBV-related hepatocellular carcinoma development in males. Clin. Cancer Res. 17, 5593-5603.

Kanda T., Sasaki-Tanaka R., Masuzaki R., Matsumoto N., Okamoto H. and Moriyama M. (2021). Knockdown of mitogen-activated protein kinase kinase 3 negatively regulates hepatitis A virus replication. Int. J. Mol. Sci. 22, 7420.

Kao J.H. (2008). Diagnosis of hepatitis B virus infection through serological and virological markers. Expert Rev. Gastroenterol. Hepatol. 2, 553-562.

Kulcheski F.R., Christoff A.P. and Margis R. (2016). Circular RNAs are miRNA sponges and can be used as a new class of biomarker. J. Biotechnol. 238, 42-51.

Lai E.C. (2002). Micro RNAs are complementary to 3' UTR sequence motifs that mediate negative post-transcriptional regulation. Nat. Genet. 30, 363-364.

Liaw Y.F. (2013). Impact of therapy on the long-term outcome of chronic hepatitis B. Clin. Liver Dis. 17, 413-423.

Liu B., Yang G., Wang X., Liu J., Lu Z., Wang Q., Xu B., Liu Z. and Li J. (2020). CircBACH1 (hsa_circ_0061395) promotes hepatocellular carcinoma growth by regulating p27 repression via HuR. J. Cell Physiol. 235, 6929-6941.

Livak K.J. and Schmittgen T.D. (2001). Analysis of relative gene expression data using real-time quantitative PCR and the 2(-Delta Delta C(T)) Method. Methods 25, 402-408.

Neuveut C., Wei Y. and Buendia M.A. (2010). Mechanisms of HBV-related hepatocarcinogenesis. J. Hepatol. 52, 594-604.

Paulmurugan R. (2013). MicroRNAs - a new generation molecular targets for treating cellular diseases. Theranostics 3, 927-929.

Qu S., Yang X., Li X., Wang J., Gao Y., Shang R., Sun W., Dou K. and Li H. (2015). Circular RNA: A new star of noncoding RNAs. Cancer Lett. 365, 141-148.

Shi T., Hua Q., Ma Z. and Lv Q. (2017). Downregulation of miR-200a-3p induced by hepatitis B Virus X (HBx) Protein promotes cell proliferation and invasion in HBV-infection-associated hepatocarcinoma. Pathol. Res. Pract. 213, 1464-1469.

Shi C., Yang Y., Zhang L., Yu J., Qin S., Xu H. and Gao Y. (2019). MiR-200a-3p promoted the malignant behaviors of ovarian cancer cells through regulating PCDH9. Onco. Targets Ther. 12, 8329-8338.

Song K., Han C., Zhang J., Lu D., Dash S., Feitelson M., Lim K. and Wu T. (2013). Epigenetic regulation of MicroRNA-122 by peroxisome proliferator activated receptor-gamma and hepatitis b virus X protein in hepatocellular carcinoma cells. Hepatology 58, 1681-1692.

Song M., Xia L., Sun M., Yang C. and Wang F. (2018). Circular RNA in Liver: Health and diseases. Adv. Exp. Med. Biol. 1087, 245-257.

Sun D., Zhu L., Yao D., Chen L., Fu L. and Ouyang L. (2018). Recent progress in potential anti-hepatitis B virus agents: Structural and pharmacological perspectives. Eur. J. Med. Chem. 147, 205-217.

Tajik Z., Keyvani H., Bokharaei-Salim F., Zolfaghari M.R., Fakhim S., Keshvari M. and Alavian S.M. (2015). Detection of hepatitis B virus covalently closed circular DNA in the plasma of Iranian HBeAg-negative patients with chronic hepatitis B. Hepat. Mon. 15, e30790.

Tak H., Kang H., Ji E., Hong Y., Kim W. and Lee E.K. (2018). Potential use of TIA-1, MFF, microRNA-200a-3p, and microRNA-27 as a novel marker for hepatocellular carcinoma. Biochem. Biophys. Res. Commun. 497, 1117-1122.

Tharayil V.S. and Roberts L.R. (2006). Molecular targets for therapy of hepatitis B virus-induced hepatocellular carcinoma. Minerva Gastroenterol. Dietol. 52, 387-406.

Wang Y. and Wen F. (2020). MicroRNA-335 inhibits the growth, chemosensitivity, and metastasis of human breast cancer cells by targeting MAP3K2. J. BUON 25, 666-674.

Wang C.M., Wang Y., Fan C.G., Xu F.F., Sun W.S., Liu Y.G. and Jia J.H. (2011). miR-29c targets TNFAIP3, inhibits cell proliferation and induces apoptosis in hepatitis B virus-related hepatocellular carcinoma. Biochem. Biophys. Res. Commun 411, 586-592.

Wang M., Lv G., Jiang C., Xie S. and Wang G. (2019). miR-302a inhibits human HepG2 and SMMC-7721 cells proliferation and promotes apoptosis by targeting MAP3K2 and PBX3. Sci. Rep. 9, 2032.

Wang S., Cui S., Zhao W., Qian Z., Liu H., Chen Y., Lv F. and Ding H.G. (2018). Screening and bioinformatics analysis of circular RNA expression profiles in hepatitis B-related hepatocellular carcinoma. Cancer Biomark. 22, 631-640.

Wang M., Gu B., Yao G., Li P. and Wang K. (2020). Circular RNA expression profiles and the pro-tumorigenic function of circRNA_10156 in bepatitis B virus-related liver cancer. Int. J. Med. Sci. 17, 1351-1365.

Xie K.L., Zhang Y.G., Liu J., Zeng Y. and Wu H. (2014). MicroRNAs associated with HBV infection and HBV-related HCC. Theranostics 4, 1176-1192.

Xiong D.D., Dang Y.W., Lin P., Wen D.Y., He R.Q., Luo D.Z., Feng Z.B. and Chen G. (2018). A circRNA-miRNA-mRNA network identification for exploring underlying pathogenesis and therapy strategy of hepatocellular carcinoma. J. Transl. Med. 16, 220.

Yu J., Ding W.B., Wang M.C., Guo X.G., Xu J., Xu Q.G., Yang Y., Sun S.H., Liu J.F., Qin L.X., Liu H., Yang F. and Zhou W.P. (2020). Plasma circular RNA panel to diagnose hepatitis B virus-related hepatocellular carcinoma: A large-scale, multicenter study. Int. J. Cancer 146, 1754-1763.

Yuen M.F., Chen D.S., Dusheiko G.M., Janssen H.L.A., Lau D.T.Y., Locarnini S.A., Peters M.G. and Lai C.L. (2018). Hepatitis B virus infection. Nat. Rev. Dis. Primers 4, 18035.

Zang Y., Tai Y., Wan B. and Jia X. (2016). miR-200a-3p promotes the proliferation of human esophageal cancer cells by post-transcriptionally regulating cytoplasmic collapsin response mediator protein-1. Int. J. Mol. Med. 38, 1558-1564.

Zhang L. and Wang Z. (2020). Circular RNA hsa_circ_0004812 impairs IFN-induced immune response by sponging miR-1287-5p to regulate FSTL1 in chronic hepatitis B. Virol. J. 17, 40.

Zhang Y., Wang D., Zhu T., Yu J., Wu X., Lin W., Zhu M., Dai Y. and Zhu J. (2021). CircPUM1 promotes hepatocellular carcinoma progression through the miR-1208/MAP3K2 axis. J. Cell Mol. Med. 25, 600-612.

Zhu K., Wang L., Zhang X., Sun H., Chen T., Sun C., Zhang F., Zhu Y., Yu X., He X. and Su Y. (2021). LncRNA HCP5 promotes neuroblastoma proliferation by regulating miR-186-5p/MAP3K2 signal axis. J. Pediatr. Surg. 56, 778-787.

Accepted March 30, 2022